Planar Lipid Bilayers (BLMs) and their Applications
H.T. Tien and A. Ottova-Leitmannova (Editors)

Chapter 5

Elastic properties of bilayer lipid membranes and pore formation

Dumitru Popescu[a,b], Stelian Ion[b], Aurel Popescu[c@], and Liviu Movileanu[d]

[a]Laboratory of Biophysics, University of Bucharest, Faculty of Biology, Splaiul Independentei 91-95, Bucharest R-76201, Romania

[b]Institute of Applied Mathematics, Calea 13 Septembrie 13, P.O.Box 1-24, Bucharest, Romania

[c]Department of Electricity and Biophysics, University of Bucharest, Faculty of Physics, Bucharest-Magurele, P.O.Box MG-11, R-76900, Romania

[d]Department of Medical Biochemistry and Genetics, The Texas A&M University System Health Science Center, 440 Reynolds Medical Building, College Station, Texas 77843-1114, USA

1. INTRODUCTION

Phospholipid bilayer membranes (BLM's) represent a useful model system to examine fundamental aspects of the lipid bilayer components of biological cell membranes and, particularly, to investigate their elastic properties. They are self-assembled structures of amphipatic molecules with physical features closely similar to those of smectic liquid crystals [1]. Lipid bilayer matrix is capable of incorporating both hydrophobic and amphipatic molecules like proteins, other lipids, peptides, steroids and cosurfactants. The elastic properties of lipid membranes regarded as continuous media have been used in a variety of studies ranging from local phenomena, such as lipid-lipid [1-11], lipid-protein [12-25] and protein-protein interactions [26-27], to shape fluctuations of the whole cells [28-32]. In addition, the liquid hydrocarbon nature of the bilayer is maintained by inter-molecular interactions between phospholipids at nanoscopic scale: electrostatic and dipole-dipole interactions between the polar headgroups [33, 34], interactions mediated by water molecules [35], and van der Waals dispersion interactions between hydrocarbon chains [36-38].

[@]The correspondence author. Fax: +(331) 69 075 327; +(401) 4 208 625;
E-mails: Aurel.Popescu@curie.u-psud.fr; p.aurel@mailbox.ro

The surfaces of a BLM are neither perfectly planar nor rigid [39, 40]. The BLM system is a quasi-two-dimensional flexible structure that undergoes continuously a variety of conformational and dynamic transitions [41-44]. Furthermore, the artificial and natural BLMs are not insulating systems, but permeable for water and electrolytes that diffuse across by a diversity of transmembrane pores.

Stochastic transmembrane pores are generated by either of the following mechanisms: random and biased thermal fluctuations (thermoporation), and electrical triggering (electroporation). Lipid molecules inside BLM follow three distinct categories of random thermal movements: lateral translations, parallel to the bilayer surface, with the lateral diffusion coefficient in the order of 10^{-7} m^2s^{-1} (D_l) [45], oscillations and rotations around the lipid axes perpendicularly to the bilayer surface [46].

Lateral translations with random directions induce local fluctuations of the density of the lipid polar headgroups at bilayer surfaces. Therefore, a snapshot of the bilayer surface reveals local domains of nanoscopic dimension with a higher density of polar headgroups (i.e. clusters) as well as zones with a lower density. For certain physical conditions of BLM (pH, temperature, lipid components, electrochemical potential, etc.), the latter zones represent small local defects (i.e. vacancies) of the membrane. In these domains, the water molecules can penetrate the hydrophobic matrix of the bilayer. Let us consider the case of two independent defects from each monolayer that are aligned in a perpendicular direction on the membrane surface. They can generate a cylindrical hydrophobic pore with the inner surface flanked by the hydrophobic chains of the lipids. Therefore these types of transient pores are of hydrophobic nature. It is also possible that the polar headgroups, situated in the proximity of a hydrophobic pore to obey rotations towards its interior. In this case, the internal hydrophobic surface of the pores will become coated with polar headgroups. Thus, these pores have a hydrophilic nature, have no more a cylindrical geometry and have more stability than the hydrophobic ones [47]. In other words, the random thermal fluctuations of the polar headgroup density in the two monolayers of BLM are able to generate stochastic transmembrane pores.

The presence of hydrophobic thickness fluctuations inside BLM was demonstrated both by theory [3] and experiment. This was achieved by determination of the values of bilayer thickness (h) from three independent procedures: electrical capacitance measurements (h_c) [48], optical reflectance measurements (h_r) [49, 50], and direct computation (h_{av}). Tanford (1980) [44] calculated the bilayer thickness using the following formula $h_{av} = N_l M/\rho$, where N_l, M and ρ are the number of lipids per unit area, the molecular weight of the hydrophobic chains and the density of the hydrophobic zone, respectively. Because of the "thickness fluctuations" of the hydrophobic regions, h_c should be equal to h_{av}, while, in this case, both of them should be smaller than h_r by the thickness of the polar layer (h_{tp}): $h_c \cong h_{av} = h_r - h_{tp}$. If the lipid bilayer would have

a uniform thickness, then h_c should be equal to h_{av}. In the case of BLM composed by a binary mixture of lipids, a selective association between phospholipids takes place following appearance of phospholipid domains. Their thickness is dependent on the length of the hydrocarbon chain of lipid components [51-55]. Popescu et al. (1991) [56] demonstrated the appearance of stochastic pores in BLMs due to fluctuations in bilayer thickness. The height of the energy barrier for membrane perforation following such a mechanism is large though (about 91 kT, where k and T are the Boltzmann constant and absolute temperature, respectively). In this case, the geometrical profile of the pore is of an elliptical toroidal form. It was also shown that such a transmebrane pore could evolve to a stable state [56]. The results obtained by this model were pretty surprising, because of the rapid time scale for closure of statistical pores in membranes. Two years latter on, Zhelev and Needham (1993) [57] have created large, quasistable pores in lipid bilayer vesicles, thus keeping with the previous model prediction [56]. The membrane's resistance to rupture [58, 59] in terms of a line tension for a large pore in bilayer vesicles was calculated by Moroz and Nelson (1997) [60].

Stochastic transmembrane pores can also be formed by biased thermal motion of lipids [42]. This mechanism is sometimes called thermoporation. The pores appear in the membrane via a thermally induced activation process. Alternatively, the activation process for pore formation can be induced via an external electrical field (also, called electroporation) [61, 62]. The pore generated by electroporation is larger and more stable [63]. The electroporation mechanism was proposed for delivery of drugs and genes to cells and tissues [61, 62, 64].

Transmembrane protein pores are formed by proteinaceous systems covering a wide range from small peptide channels (e.g. gramicidin, alamethicin, melittin etc.) to large protein multimeric assembled channels. Since these pores are large and water-filled, the hydrophilic substances, including ions, can diffuse across them, thus dissipating the membrane electrical potential. Transmembrane protein pores are consisted of integral proteins from two major structural classes: (1) selective channels formed by bundled transmembrane α-helical structures, and (2) selective channels, pores and porins formed by monomeric (e.g. OmpG), dimeric (e.g. selective Cl^- channels), trimeric (e.g. OmpF) or multimeric transmembrane β-barrel structures (e.g. α-hemolysin, leukocidins, cytolysins) [65]. The lipid bilayer may be used as an *in vitro* system to study these protein channels when they are reconstituted into a functional membrane [66]. In addition, the BLMs can be used as a tool for membrane protein engineering and its applications in either single-molecule biophysics [67-70] or biotechnological area [68].

In another example, colicin Ia, a protein secreted by *Escherichia coli*, forms voltage-gated ion channels both in the inner membrane of target bacteria and in planar BLMs [71-73]. Colicin Ia is a membrane transporter belonging to

the class of bacterial toxins that share the same strategy: they are inserted into the membrane of the other nutrient competing bacteria, thus generating pores of large dimensions. Accordingly, these pores will damage the electrochemical membrane potential and, finally, will provoke the death of these competing bacteria. As compared with the stochastic pores mentioned above, the proteinaceous pores have a different mechanism of formation and also different properties. While a stochastic pore "forgets" its mechanism of generation, some of the transmembrane protein pores (e.g. colicin Ia) seem to exhibit "memory" effects, at least under the influence of a specific sequence of pulses used for BLM electrical stimulation [74].

Genetic pores were encountered in the wall of sinusoid vessels from the mammalian liver. The endothelial cells of these vessels have numerous sieve plate pores [75]. These pores of about 0.1 μm diameter enable a part of blood plasma and chylomicrons to pass from sinusoidal space into the space of Disse. Therefore, the endothelial pores control the exchange of fluids, solutes and particles between the sinusoidal blood and the space of Disse [75, 76].

In this work, we used the elasticity theory of continuous media to describe the appearance of stochastic pores across planar BLMs.

2. BLMs – SMECTIC LIQUID CRYSTALS

Phospholipids possess a very exciting feature – the amphiphilic nature, that is, they have a hydrophobic and hydrophilic character due to their hydrocarbon chains and polar headgroups, respectively. Therefore, if the phospholipids are dissolved in a strong polar medium (e.g. water), they spontaneously aggregate into ordered structures: planar lipid bilayers or spherical vesicles. In these ordered structures the polar headgroups have the orientation towards the exterior of the bilayer (i.e. towards the polar medium, in this case, water), while the hydrocarbon chains tend to be hidden into hydrophobic interior, thus avoiding a direct contact with the polar medium [44, 77, 78].

If the planar bilayer membranes are analysed only from the point of view of their physical properties, one can find out:

1. their component molecules are oriented along a preferential direction, almost perpendicularly to the BLM surface;
2. the two monolayers have closely similar thickness and can glide one along to another;
3. there is no exchange of molecules between the two monolayers. Translocation events from one monolayer to another (e.g. flip-flop transitions) are very improbable processes (see the section 8 of this chapter). The flip-flop diffusion coefficient (D_{ff}) is in the order of 10^{-23} m^2s^{-1}, which is much smaller than D_l [45];

4. in each monolayer there is a short range order, which is characteristic to the liquids. This is because both the interactions between the polar headgroups and those of van der Waals-London nature between the hydrophobic chains are known to be of short range;

5. the bilayer possesses a unique optical axis, *Oz*, perpendicularly to the bilayer plane;

6. the two orientations, *Oz* and *–Oz*, perpendicularly to the bilayer surface are equivalent;

These properties are characteristic to a smectic liquid crystal of type A [79].

The X-rays diffraction diagrams [80] and the analysis of the thermal phase transitions [81, 82] suggest a special BLM architecture in the case of the bilayers composed of lipids whose chains differ by more than four methylene groups. In this BLM structural organization, the phospholipid hydrocarbon chains are positioned so that the shorter molecules of one monolayer are aligned along with the longer molecules of the other one, and vice versa. Both of these molecules are tilted over the bilayer surfaces. These peculiar structures seem to be unstable. They appear only in the case of an adequate tilting of the support walls used to form the bilayer. Even in this case the lipid bilayer is a liquid crystal, but of the type C.

The mesomorph state of BLM, considered as a smectic liquid crystal of the type A, allows the application of both experimental and theoretical methods that are specific for the study of liquid crystals.

3. DEFORMATION FREE ENERGY OF BLM

In 1974, Pierre G. de Gennes was first that applied the theory of elasticity of continuous media to liquid crystals [79]. Taking into account a single axis liquid crystal, the average orientation of the long molecular axis is described in the point r by the direction vector $\boldsymbol{n(r)}$. The direction of $\boldsymbol{n(r)}$ coincides with the optical axis of the liquid crystal. In the first part of this approach, we shall consider that the elastic deformations do not induce local modifications of the liquid crystal density.

Let us consider a rectangular system of coordinates *Oxyz*, in which $\boldsymbol{n(r)}$ is parallel to the *Oz* axis. Also, let us consider the case of small deformations. The components of the direction vector $\boldsymbol{n(r)}$ can be equated by the following Taylor series:

$$\begin{aligned} n_x &= n_{x0} + e_1 x + e_2 y + e_3 z + O(r^2) \\ n_y &= n_{y0} + e_4 x + e_5 y + e_6 z + O(r^2) \\ n_z &= 1 + O(r^2) \end{aligned} \qquad (1)$$

where deformation coefficients e_i (i=1÷6) as well as the deformation types from the Eqs. (1) are the following:

$$e_1 = \frac{\partial n_x}{\partial x} \quad ; \quad e_5 = \frac{\partial n_y}{\partial y} \qquad (\textit{the splay distorsion})$$

$$e_2 = \frac{\partial n_x}{\partial y} \quad ; \quad e_4 = -\frac{\partial n_y}{\partial x} \qquad (\textit{the twist distorsion}) \qquad (2)$$

$$e_3 = \frac{\partial n_x}{\partial z} \quad ; \quad e_6 = \frac{\partial n_y}{\partial z} \qquad (\textit{the bend distorsion})$$

and $O(r^2)$ are terms of the order of magnitude of r^2.

The free energy density is a quadratic form of the deformation coefficients:

$$F(x,y,z) = F_0 + \sum_{i=1}^{6} k_i e_i + \frac{1}{2}\sum_{i=1}^{6}\sum_{j=1}^{6} k_{ij} e_i e_j \qquad (3)$$

where F_0 denotes the free energy of the initial non-deformed state. k_i and k_{ij} are coefficients that will be discussed later on.

Due to special properties of the single axis liquid crystals, the expression of the free energy density is invariant to any rotation around the Oz axis and, also to the inversion $z \rightarrow -z$ (Oz is equivalent to $-Oz$, as we already stated above). If the surface energy is considered to be negligible too, then only three independent coefficients k_{ij} will remain in Eq. (3). They will be renamed as follows: $k_{11}=K_1$, $k_{22}=K_2$, $k_{33}=K_3$. In this way, the variation of the free energy, ΔF, derived from the expression (3), will have a simpler form:

$$\Delta F(x,y,z) = \frac{1}{2}K_1(\text{div }\mathbf{n})^2 + \frac{1}{2}K_2(\mathbf{n}\cdot\text{curl}\,\mathbf{n})^2 + \frac{1}{2}K_3(\mathbf{n}\times\text{curl}\,\mathbf{n})^2 \qquad (4)$$

This is the fundamental expression of the theory of the continuous elastic media applied to liquid crystals. The crystal deformation is characterised by the ***n(r)***. Its modulus is unity. However, it has a variable direction unlike a unit vector. We also assume that ***n*** varies slowly and smoothly with ***r***. The coefficients K_i (i = 1, 2, 3) are positive elastic constants that correspond to each type of deformations. In Eq. (4), the first, second and third terms indicate the splay free energy, the torsion free energy (twist deformation) and the bending free energy, respectively.

Let us take into account a smectic liquid crystal of the type A, which is composed of many parallel and equidistant layers. The thickness of a layer is denoted by h. The component molecules with an elongated conformation have their long axes perpendicularly oriented to the layer surfaces. The system of ordinates has its origin in the mass centre of the liquid crystal with the axis Oz oriented perpendicularly on the layer surfaces. Let us assume that the liquid crystal undergoes a small deformation, which is characterised by a long

wavelength. The shift of the n-th layer, in the direction Oz, as a consequence of this small deformation, is denoted by $w_n\ (x, y)$. If the crystal is considered a continuous medium, then the discrete variable n can be converted in a continuous variable $z = nh$. Accordingly, $w_n\ (x, y)$ will be replaced by $w(x, y, z)$. Following this deformation, the liquid crystal molecules have their long axis no longer parallel to Oz. In the particular case of a large wavelength deformation, one can consider that the molecular deviations versus Oz could be small, and therefore neglected. To take into consideration the BLM thickness fluctuations, we implemented the compression deformations as well. Therefore, a local change in the liquid crystal density, ρ, will be generated:

$$\rho = \rho_0(1-\psi(\mathbf{r})) \tag{5}$$

where ρ and ρ_0 are the layer densities in the presence and absence of compression deformation, respectively. Here, $\psi(r)$ is a function expressing the volume compression.

To find out an explicit form of the compression deformation, we consider the function $\psi(r)$ split in two terms:

$$\psi(\mathbf{r}) = \theta(\mathbf{r}) + \beta(\mathbf{r}) \tag{6}$$

The first and second term accounts for the compression parallel and perpendicularly oriented to the liquid crystal layer surfaces, respectively. Thus, one can express the volume compression as a function depending on the transversal compression by means of the parameter $\beta(r)$. This is also described as a function depending on $w(r)$: $\beta(r) = \partial w/\partial z$.

In the case of smectic liquid crystal of the type A, both torsion and bending deformations are excluded. Therefore, the last two terms of the Eq. (4) are cancelled. However, if the compression deformation is taken into consideration, then the Eq. (4) is replaced by the following:

$$\Delta F(x, y, z) = \frac{1}{2} K_1(\operatorname{div}\mathbf{n})^2 + A\theta^2 + B\beta^2 + 2C\beta\theta \tag{7}$$

where A and B are the compression coefficients for parallel and perpendicular directions to the liquid crystal layers, respectively. C is an interaction constant between the two types of compressions.

From the stability condition ($A \times B > C^2$) and static equilibrium ($\Delta F = 0$), we can obtain an expression for parameter $\theta(r)$:

$$\theta(\mathbf{r}) = -\frac{C}{A}\frac{\partial w}{\partial z} \tag{8}$$

If we take into account the compression deformation, then the free energy of deformation per unit volume of a smectic liquid crystal is the following:

$$\Delta F(x,y,z)=\frac{1}{2}\overline{B}\left(\frac{\partial w}{\partial z}\right)^2+\frac{1}{2}K_1(\operatorname{div}\mathbf{n})^2 \tag{9}$$

where

$$\overline{B}=B-\frac{C^2}{A} \tag{10}$$

Let us consider a reference domain $G=\{(x,y,z)|-h\le z\le 0,(x,y)\}\in S$ occupied by the unperturbed liquid crystal (S is an arbitrary 2D domain). We suppose that the upper boundary undergoes a deformation given by $u(x,y)$. We also consider that the bottom boundary rests unperturbed. We assume that inside the two boundaries the deformation is given by $w(x,y,z)=b(z)u(x,y)$. It is conceivable that the components of the direction vector n do not depend on z, so that its projections on the Ox and Oy axes are given by:

$$\begin{aligned} n_x &= -\frac{\partial u}{\partial x}<<1 \\ n_y &= -\frac{\partial u}{\partial y}<<1 \end{aligned} \tag{11}$$

To find out the unknown function $b(z)$, we apply the boundary conditions as well as a condition on the minimum of the free energy. Therefore, the function $b(z)$ must satisfy:

$$\begin{cases} -\dfrac{\mathrm{d}^2 b}{\mathrm{d}z^2}=0, \\ b(0)=1,\ \ b(-h)=0. \end{cases} \tag{12}$$

The solution of the problem stated above is given by:

$$b(z)=z/h+1 \tag{13}$$

Therefore, in this case the deformation free energy per unit area is:

$$\Delta F(x,y)=h\overline{B}\left(\frac{u}{h}\right)^2+hK_1\left(\frac{\partial^2 u}{\partial x^2}+\frac{\partial^2 u}{\partial y^2}\right)^2 \tag{14}$$

If we take into account the compression deformation, then the free energy of deformation per unit volume of a smectic liquid crystal is the following:

$$\Delta F(x,y,z)=\frac{1}{2}\overline{B}\left(\frac{\partial w}{\partial z}\right)^2+\frac{1}{2}K_1(\operatorname{div}\mathbf{n})^2 \tag{9}$$

where

$$\overline{B}=B-\frac{C^2}{A} \tag{10}$$

Let us consider a reference domain $G=\{(x,y,z)\,|\,-h\le z\le 0,(x,y)\in S\}$ occupied by the unperturbed liquid crystal (S is an arbitrary 2D domain). We suppose that the upper boundary undergoes a deformation given by $u(x,y)$. We also consider that the bottom boundary rests unperturbed. We assume that inside the two boundaries the deformation is given by $w(x,y,z)=b(z)u(x,y)$. It is conceivable that the components of the direction vector $\boldsymbol{n}$ do not depend on z, so that its projections on the Ox and Oy axes are given by:

$$\begin{aligned} n_x &= -\frac{\partial u}{\partial x}<<1 \\ n_y &= -\frac{\partial u}{\partial y}<<1 \end{aligned} \tag{11}$$

To find out the unknown function $b(z)$, we apply the boundary conditions as well as a condition on the minimum of the free energy. Therefore, the function $b(z)$ must satisfy:

$$\begin{cases} -\dfrac{\mathrm{d}^2 b}{\mathrm{d}z^2}=0, \\ b(0)=1,\quad b(-h)=0. \end{cases} \tag{12}$$

The solution of the problem stated above is given by:

$$b(z)=z/h+1 \tag{13}$$

Therefore, in this case the deformation free energy per unit area is:

$$\Delta F(x,y)=h\overline{B}\left(\frac{u}{h}\right)^2+hK_1\left(\frac{\partial^2 u}{\partial x^2}+\frac{\partial^2 u}{\partial y^2}\right)^2 \tag{14}$$

The variation of the unit area Δs, due to the BLM deformation, is given by:

$$\Delta s = \left[1+\left(\frac{\partial u}{\partial x}\right)^2+\left(\frac{\partial u}{\partial y}\right)^2\right]^{1/2} - 1 \cong \frac{1}{2}\left[\left(\frac{\partial u}{\partial x}\right)^2+\left(\frac{\partial u}{\partial y}\right)^2\right] \tag{15}$$

Let us consider the surface tension coefficient denoted by γ. Taking into account the energetic contribution due to the change in the cross-sectional area of the BLM surface, one can obtain a complete expression for the deformation free energy per unity area:

$$\Delta F(x,y) = h\bar{B}\left(\frac{u}{h}\right)^2 + hK_1\left(\frac{\partial^2 u}{\partial x^2}+\frac{\partial^2 u}{\partial y^2}\right)^2 + \gamma\left[\left(\frac{\partial u}{\partial x}\right)^2+\left(\frac{\partial u}{\partial y}\right)^2\right] \tag{16}$$

In this formula, the first term represents the elastic compression energy of the BLM, which is characterized by the compression elastic constant, $\bar{B}$. The second term indicates the elastic energy of splay distortion, which is characterized by the elastic coefficient, K_1. The third term is the free energy due to the surface tension, which is characterised by the surface tension coefficient, γ.

In our case, the deformation of a monolayer obey to a cylindrical symmetry, so that Eq. (14) can simply be written in a system of polar ordinates:

$$\Delta F(r) = \bar{B}\frac{u^2}{h} + hK_1\left(\frac{\partial u}{r\partial r}+\frac{\partial^2 u}{\partial r^2}\right)^2 + \gamma\left(\frac{\partial u}{\partial r}\right)^2 \tag{17}$$

Therefore, the total free energy of BLM deformation on a planar surface perturbation of radius, R, is given by:

$$\Delta\bar{F} = 2\pi\int_0^R\left[\bar{B}\frac{u^2}{h} + hK_1\left(\frac{\partial u}{r\partial r}+\frac{\partial^2 u}{\partial r^2}\right)^2 + \gamma\left(\frac{\partial u}{\partial r}\right)^2\right]rdr \tag{18}$$

4. PORE FORMATION DUE TO BLM THICKNESS FLUCTUATIONS

In the next section of this chapter, we consider only the oscillations that are perpendicularly oriented to the bilayer surface. There are the following interactions between phospholipids: (a) between the polar headgroups, (b) between the polar headgroups and the hydrophobic chains, and (c) between hydrophobic chains. Individual motions of the phospholipids are transformed in

a collective thermal motion normally to the BLM surface. This phenomenon can trigger local changes in the BLM thickness. Here, we would like to address the following question: can these collective motions themselves induce the BLM perforations?

We consider only a local surface perturbation, $u(r)$, with a wavelength, λ, and its amplitude equal to half of bilayer thickness, h:

$$u(r) = -h\cos\frac{2\pi r}{\lambda} \tag{19}$$

The elasticity theory, applied to the lipid bilayer regarded as continuous media, has a great advantage because it takes into account the intrinsic properties of bilayer membrane (e.g. the constants $\overline{B}$, K_1 and γ). This was the main reason why we have used the elasticity theory to calculate the BLM free energy, ΔF, induced by a surface perturbation. In fact, we want to demonstrate that the thermal movements of the phospholipids, normally oriented to the BLM surfaces, can produce such thickness fluctuations that trigger the pore formation.

The initial state of the BLM was considered that in which its molecules do not move at all (i.e. we consider the initial temperature 0 K). At this temperature, both surfaces of the BLM are planar. By warming the BLM up to the temperature T > 0 K, the phospholipid molecules will get kinetic energies and their thermal motions will start deforming the lipid bilayer. This phenomenon favours the appearance of thickness fluctuations. Thus, this thermal energy must be equal or greater than the free energy of deformation:

$$\frac{a}{\pi R^2}\Delta\overline{F} \le (3N - N_g)\frac{kT}{2} \tag{20}$$

where N is the number of atoms of a single molecule, N_g is the number of chemical intra-molecular bonds, a represents the cross-sectional area of the polar headgroups [83] and k is the Boltzmann constant. For the sake of simplicity, we have chosen the case for which $3N - N_g = 6$.

We are interested to find the parameters λ and R that satisfy the following relation:

$$\frac{2a}{R^2}\int_0^R rF(r,\lambda)dr = (3N - N_g)\frac{kT}{2} \tag{21}$$

After somehow tedious calculus, the last equation can be written as:

$$a_0(y)x^4 + b_0(y)x^2 + c_0(y) = 0 \tag{22}$$

where the variables x and y and the functions a_0, b_0, c_0 are given by:

$$x = h\frac{2\pi}{\lambda},\ y = R\frac{2\pi}{\lambda}$$

$$a_0(y) = \frac{K_1}{Bh^2}\left(1 + \frac{\sin 2y}{y} - 3\frac{\cos 2y - 1}{2y^2} + \frac{4}{y^2}\int_0^1 \frac{\sin^2 ty}{t}dt\right)$$

$$b_0(y) = \frac{\gamma}{Bh}\left(1 - \frac{\sin 2y}{y} - \frac{\cos 2y - 1}{2y^2}\right)$$

$$c_0(y) = 1 + \frac{\sin 2y}{y} + \frac{\cos 2y - 1}{2y^2} - (3N - N_g)\frac{kT}{Bha} \tag{23}$$

Unfortunately the Eq. (22) is too complicated to easily obtain the explicit formulae for λ and R, but one can obtain their parametrical representation. We shall consider x as a unknown and y as a parameter in such a way that the equations are reduced to an algebraic equation for x. Since the functions a_0 and b_0 are always positive, the equation has real solutions only if the function c_0 is negative. If these conditions are fulfilled, we get only one positive solution of Eq. (22):

$$\lambda(y) = 2\pi h\left(\sqrt{\frac{-b_0(y) + \sqrt{b_0^2(y) - 4a_0(y)c_0(y)}}{2a_0(y)}}\right)^{-1}$$

$$R(y) = \frac{y\lambda(y)}{2\pi} \tag{24}$$

It is worth mentioning that the wavelength depends on the interactions between the polar headgroups and, also, on the relative motions of the neighboured molecules. In other words, the wavelength depends on the dephasing that appears between the neighboured molecules along the radius of the BLM surface occupied by the molecules involved in the collective thermal motion. Obviously, this dephasing can be influenced by the motion of the molecules from the adjacent medium (e.g. the motion of ions and waters).

5. CALCULATION OF THE PORE RADIUS

After perforation of the BLM, a rearrangement of molecules situated in the deformation zones may take place, so that the surface of the sinusoidal torus is modifying its concavity becoming a surface of a revolution elliptic torus. By equating the volumes delimited by the two revolution surfaces (i.e. sinusoidal and ellipsoidal), before the BLM perforation and after molecular rearrangement, the pore radius can be obtained. In the next steps, we calculate these two volumes.

We consider the space domain, D, of an ellipsoidal torus, defined by the relations:

$$z \in (0,h),\ r \le \lambda/4$$
$$\frac{z^2}{h^2} + \frac{(r-\lambda/4)^2}{b^2} \le 1 \tag{25}$$

where b is a parameter that fixes the space configuration of the pore.

Using a system of polar coordinates, the volume, D, of an ellipsoidal torus, is given by:

$$V = 2\pi \iint_D r dr dz \tag{26}$$

With some standard calculations, one can obtain the following expression for V:

$$V_a(\lambda,b) = 2\pi h \begin{cases} b\left(\frac{\lambda\pi}{16} - \frac{b}{3}\right), & b \le \frac{\lambda}{4} \\ \frac{\lambda^2}{32}\sqrt{1-\left(\frac{\lambda}{4b}\right)^2} + \frac{\lambda b}{8}\arcsin\frac{\lambda}{4b} + \frac{b^2}{3}\left[\left(\sqrt{1-\left(\frac{\lambda}{4b}\right)^2}\right)^3 - 1\right], & b \ge \frac{\lambda}{4} \end{cases} \tag{27}$$

For any $R \in (\lambda/4,\ \lambda/2)$, let us define the function $f(r)$ by:

$$f(r) = \begin{cases} h\left(1-\cos\frac{2\pi}{\lambda}r\right), & r \in (0,R) \\ h\left(1-\cos\frac{2\pi}{\lambda}(2R-r)\right), & r \in (R, 2R-\lambda/4) \end{cases} \tag{28}$$

Using this function we define the following two domains:

$$D^{\lambda} = \{(z,r) | r \in (0,\ \lambda/4),\ z \in (0, f(r))\} \tag{29}$$

and

$$D_{ext}^{\lambda,R} = \{(z,r) | r \in (\lambda/4, 2R-\lambda/4),\ z \in (h, f(r))\} \tag{30}$$

For $R \in (0,\ \lambda/4)$ we define also other two domains:

$$D_{\text{int}}^{\lambda,R} = \{(z,r) | r \in (0,R),\ z \in (0, f(r))\} \tag{31}$$

and

$$G_{\text{int}}^{\lambda,R} = \{(z,r) | r \in (R, \lambda/4),\ z \in (0,h)\} \tag{32}$$

Finally, we define the domain $\Omega^{\lambda,R}$ by:

$$\Omega^{\lambda,R} = \begin{cases} D^{\lambda} \cup D_{ext}^{\lambda,R}, & R \ge \lambda/4 \\ G_{\text{int}}^{\lambda,R} \cup D_{\text{int}}^{\lambda,R}, & R \le \lambda/4 \end{cases} \tag{33}$$

$$z\in(0,h),\ r\le\lambda/4$$
$$\frac{z^2}{h^2}+\frac{(r-\lambda/4)^2}{b^2}\le 1 \tag{25}$$

where b is a parameter that fixes the space configuration of the pore.

Using a system of polar coordinates, the volume, D, of an ellipsoidal torus, is given by:

$$V=2\pi\iint_D rdrdz \tag{26}$$

With some standard calculations, one can obtain the following expression for V:

$$V_a(\lambda,b)=2\pi h\begin{cases} b\left(\dfrac{\lambda\pi}{16}-\dfrac{b}{3}\right), & b\le\dfrac{\lambda}{4} \\ \dfrac{\lambda^2}{32}\sqrt{1-\left(\dfrac{\lambda}{4b}\right)^2}+\dfrac{\lambda b}{8}\arcsin\dfrac{\lambda}{4b}+\dfrac{b^2}{3}\left[\left(\sqrt{1-\left(\dfrac{\lambda}{4b}\right)^2}\right)^3-1\right], & b\ge\dfrac{\lambda}{4}\end{cases} \tag{27}$$

For any $R\in(\lambda/4,\ \lambda/2)$, let us define the function $f(r)$ by:

$$f(r)=\begin{cases} h\left(1-\cos\dfrac{2\pi}{\lambda}r\right), & r\in(0,R) \\ h\left(1-\cos\dfrac{2\pi}{\lambda}(2R-r)\right), & r\in(R,2R-\lambda/4)\end{cases} \tag{28}$$

Using this function we define the following two domains:

$$D^{\lambda}=\{(z,r)\,|\,r\in(0,\lambda/4),\ z\in(0,f(r))\} \tag{29}$$

and

$$D_{ext}^{\lambda,R}=\{(z,r)\,|\,r\in(\lambda/4,2R-\lambda/4),\ z\in(h,f(r))\} \tag{30}$$

For $R\in(0,\lambda/4)$ we define also other two domains:

$$D_{\text{int}}^{\lambda,R}=\{(z,r)\,|\,r\in(0,R),\ z\in(0,f(r))\} \tag{31}$$

and

$$G_{\text{int}}^{\lambda,R}=\{(z,r)\,|\,r\in(R,\lambda/4),\ z\in(0,h)\} \tag{32}$$

Finally, we define the domain $\Omega^{\lambda,R}$ by:

$$\Omega^{\lambda,R}=\begin{cases} D^{\lambda}\cup D_{ext}^{\lambda,R}, & R\ge\lambda/4 \\ G_{\text{int}}^{\lambda,R}\cup D_{\text{int}}^{\lambda,R}, & R\le\lambda/4\end{cases} \tag{33}$$

The volume of the domain $\Omega^{\lambda,R}$, characterising a sinusoidal torus, is given by:

$$V_t(\lambda,R)=2\pi h\left(\frac{\lambda}{2\pi}\right)^2\begin{cases}\dfrac{\pi^2}{8}+1-\cos\dfrac{2\pi R}{\lambda}-\dfrac{2\pi R}{\lambda}\sin\dfrac{2\pi R}{\lambda}, & R\le\dfrac{\lambda}{4}\\ \dfrac{\pi^2}{8}+1-\dfrac{\pi}{2}+\dfrac{4\pi R}{\lambda}\left(1-\sin\dfrac{2\pi R}{\lambda}\right), & R\ge\dfrac{\lambda}{4}\end{cases} \tag{34}$$

Equating the two volumes given by the Eqs. (27) and (34), namely $V_a(\lambda,b)=V_t(\lambda,R)$, one can calculate the magnitude of the pore radius r.

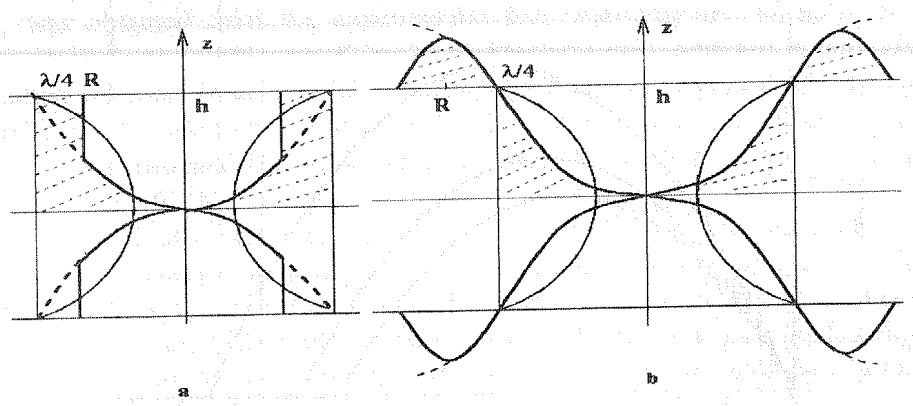

Fig. 1. Cross-sectional view through the BLM deformed in the case in which the radius, R, of the perturbation zone is: a) smaller than $\lambda/4$, and b) greater than $\lambda/4$. The forms of the pores are sketched, just immediately after the BLM perforation. h is the half of the BLM thickness. As a consequence of the lipid rearrangement (situated in the hatched zones), the molecules from the sinusoidal torus ($\Omega^{\lambda,R}$ domain) will be found in the volume limited by the elliptical surface of the ellipsoidal torus (D domain).

6. PORE FORMATION BY LATERAL THERMAL TRANSLATIONS

As stated above, when two defects, created due to lateral thermal translations, are aligned on the same perpendicular axis on both bilayer surfaces, they can generate cylindrical hydrophobic pores. Furthermore, these defects can vanish or extend towards the interior of the hydrophobic zones. Simultaneously, rotations of the phospholipids may appear, so that their polar groups cover the hydrophobic surface of the newly formed defect. In this way, the hydrophilic pores are generated as a consequence of random, but permanent thermal motions.

One can simply consider that the variation of the free energy, after a single-pore formation, contains two terms. The first term represents an energy decrease due to disappearance of a BLM surface (occupied by the pore). The second term represents an energy increase due to the pore contour generation

(so-called edge energy). Therefore, the BLM free energy associated with a single-pore formation of radius r is the following [84, 85]:

$$\Delta F = 2\pi r\sigma - \pi\gamma r^2 \tag{35}$$

where γ represents a surface tension coefficient. σ is the strain energy per unit length of the pore edge.

The two coefficients are related by the formula: $\gamma = 2h\sigma$, where $2h$ indicates the hydrophobic width of the BLM.

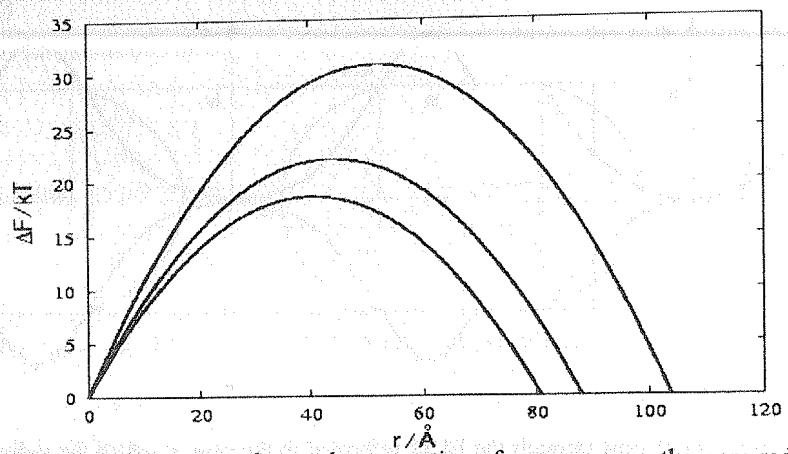

Fig. 2. The BLM free energy due to the generation of a pore versus the pore radius r. The hydrophobic width of the BLM is $2h$: 40.4 Å *(lower curve)*, 44 Å (*middle curve*), and 52 Å (*upper curve).*

According to this model, there is a critical energetic barrier $\Delta F_c = 4\pi\gamma h^2$, whether the radius r of the pore attains a critical value $r_c = 2h$ (Fig. 2). As noticed, the energy barrier value is dependent on the thickness of the hydrophobic domain and the surface tension as well, while the pore radius is equal to the bilayer thickness. If the pore radius is smaller than the critical value ($r < r_c$), then the force on the pore edge is inward and the pore tends to reseal itself. By contrast, if the pore radius is greater than this value, then the pore becomes unstable. Its diameter may increase indefinitely, thus triggering the BLM rupture.

In Fig. 2, the BLM free energy associated with the appearance of a single pore, is represented as a function of pore radius for the following values of the hydrophobic zone thickness: $2h$ = 40.4 Å, $2h$ = 44 Å, and $2h$ = 52 Å. In all the cases, $\gamma = 15\times10^{-4}$ N m^{-1}.

7. THICKNESS FLUCTUATIONS AND PORE APPEARANCE

In this section, we analyse the conditions under which the thermal fluctuations of the hydrophobic domain of the BLM, composed from single-

chain lipids, can generate transbilayer pores. In this respect, it is necessary to have information regarding the parameters from Eq. (22). Because the phospholipid membranes were extensively studied, there are sufficient data within the specific literature for required elastic constants. The thickness of the hydrophobic zone, in the case of the membrane composed of double-chain lipids is $2h$ = 40.4 Å [86]. The compressibility coefficient obtained by Hladky and Gruen [3] from the experimental data of White [87] is equal to 5.36×10^{7} Nm^{-2}.

The BLM surface area occupied by a single phospholipid is 38.6 $Å^2$, while the surface tension coefficient, γ, is $8\times10^{-4}Nm^{-1}$[88]. The splay coefficient K_1 was obtained from the experimental data regarding the modulus of the curvature elastic coefficient, $K_c = (2.8\div6.5)\times10^{-20}$J [89], obtained in the case of lecithin vesicles. Thus, from $K_1 = K_c/2h$ [1, 90] one can easily obtain the splay coefficient K_1, which is needed in Eq. (22). Because the vesicle thickness used for the experimental measurement of K_c was 30 Å, then it results that $K_1 \in (0.93\div2.17)\times10^{-11}$N.

The results presented in this section deal with the case when the deformation energy is equal to the total thermal energy of the molecules participating to the collective motion. More precisely, the results were obtained by solving the Eq. (22) in each particular case. The BLM formed by dehydrated phosphatydilcholine, with the thickness of the hydrophobic zone $2h$ = 40.4 Å, has $K_1 = 0.93\times10^{-11}$N.

One can say that the collective thermal motion of the molecules can generate three types of transbilayer pores: open stable pores, closed stable pores (zippered pores) and unstable open pores, which determine the membrane rupture. Because this approach does not imply a condition to distinguish between open, stable and unstable pores, we have used the condition obtained in the case of pores generated by surface defects induced by lateral thermal motion. Therefore, we have considered that the pores are stable, if their radius is smaller than the hydrophobic thickness of a lipid bilayer ($r < r_c = 2h$).

Generally, the wavelength bilayer deformation is a two-value function on the perturbed zone radius. There is an interval in such a way so that for each value of the R belonging to it, the solution of Eq. (22) gives two values for λ. On the other hand, the pore radius is a monotonously decreasing function on the bilayer deformation wavelength. Due to these properties of the functions $\lambda = \lambda(R)$ and $r = r(\lambda)$, for each value of R, belonging to the non-univocity domain, it is possible the formation of two pores of different sizes. The selection between these pores is made by the magnitude of deformation: that one with a smaller wavelength will cause the appearance of a smaller pore radius and vice versa.

The Tables 1-3 reflect the three characteristic features of the BLM pore formation. Their upper part comprises the parameters R, λ and r_p for the case of two pore formation, both of them open and stable; the middle part describes the case of two stable pore formation: one open pore and the other closed; the lower

part contains the values of R, λ and r_p in the case of appearance of two open pores, one stable and the other unstable.

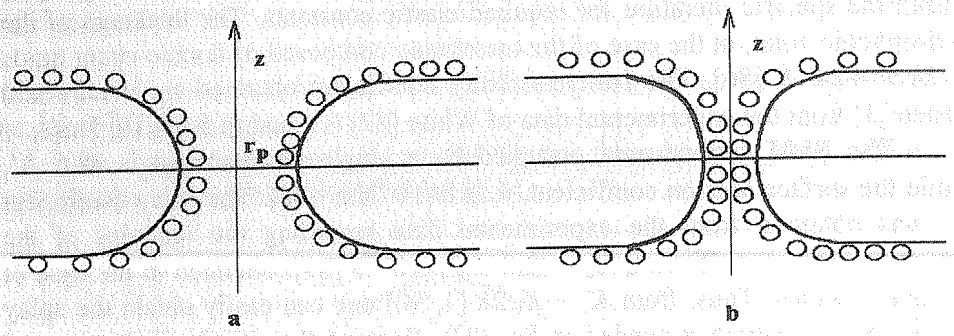

Fig. 3 The two types of pores generated by the BLM thickness fluctuations: a) open pore; b) closed pore. The circles represent the polar headgroups of the lipids. r_p is the pore radius.

In the last column of the upper part are also indicated the figures and the corresponding number associated to the curves from the figures. For an easier understanding of the tables and figures presented bellow, we describe in details the obtained data in the case of the reference BLM (Table 1 and curves 1 of the Fig.4). For each value of perturbed zone belonging to the non-univocity interval $[R_m \div R_1] = [36.0 \div 36.5]$ Å one can appear either a pore with a small radius or a pore with a large radius. If the deformation wavelength has its value in the smaller value interval $\lambda \in [\lambda_0 \div \lambda_{1m}] = [117.0 \div 112.4]$ Å, then smaller pore will appear. Its radius will be embedded into the interval: $[r_{p0} \div r_{pm}] = [10.3 \div 0.8]$ Å.

Table 1. The radia of the collective thermal motion zones of the BLM perturbation, the deformation wavelengths and the radia of the pores (or of the closing distance) in the case of reference BLM (h = 20.2 Å) and of other two BLMs differing by this one by their thickness (h = 22 Å) and their polar headgroup magnitude (a_0 = 44 Å^2). R, λ and r are measured in Å. N_m represents the minimal number of molecules which are participating to the collective thermal motion. d/h is the close ratio of the closed pores. Cv is the curve number within the Fig. 4.

	N_m	$R_m \div R_1$	$\lambda_0 \div \lambda_{1m}$	$r_{p0} \div r_{pm}$	$\lambda_0 \div \lambda_{1M}$	$r_{p0} \div r_{pM}$	Fig/Cv
h= 20.2	105	36.0-36.5	117.0-112.4	10.3-0.8	117.0-125.2	10.3-15.0	4/1
h= 22.0	137	41.0-41.6	131.4-127.7	9.6-0.3	131.4-138.4	9.6-14.6	4/3
a_0=44.0	124	41.7-42.1	132.4-129.2	8.5-0.3	132.4-138.4	8.5-13.5	4/2
	N_m	$R_1 \div R_2$	$\lambda_{1m} \div \lambda_m$	d/h	$\lambda_{1M} \div \lambda_2$	$r_{pM} \div r_{p2}$	
h= 20.2	105	36.5-37.1	112.4-111.4	0.10-0.94	125.2-130.9	15.0-16.9	
h= 22.0	137	41.6-42.3	127.7-126.8	0.21-0.95	138.4-144.8	14.6-16.8	
a_0=44.0	124	42.1-42.9	129.2-128.7	0.21-0.95	138.4-144.0	13.5-15.5	
	N_m	$R_2 \div R_c$	$\lambda_2 \div \lambda_c$	$r_{p2} \div r_{pc}$	$R_c \div R_r$	$\lambda_c \div \lambda_r$	$r_{pc} \div r_r$
h= 20.2	105	37.1-69.9	130.9-275.7	16.9-40.4	69.9- 96.4	275.7-384.1	40.4-53.1
h= 22.0	137	42.3-80.4	144.8-305.3	16.8-44.0	80.5-115.7	305.3-441.9	44.0-63.8
a_0=44.0	124	42.9-77.3	144.0-286.7	15.5-40.4	77.3-121.3	286.7-452.7	40.4-56.1

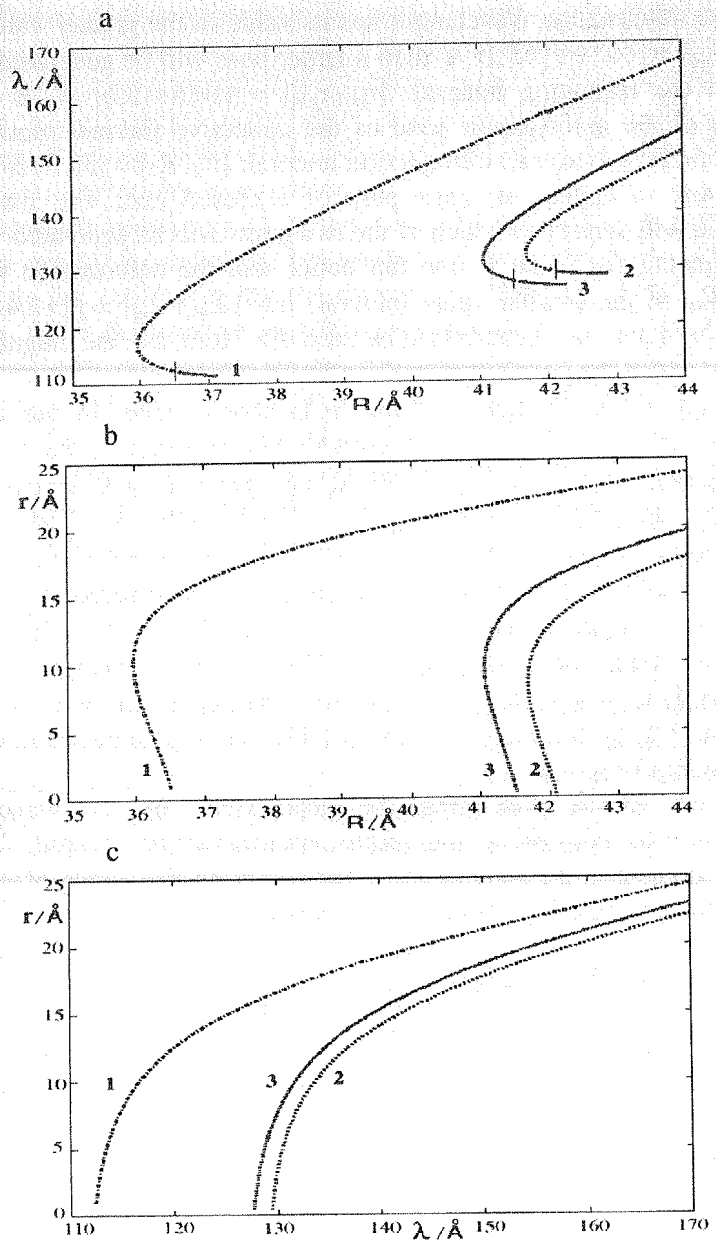

Fig. 4 The graphs, for: the deformation wavelength dependence of the perturbation zone radius (a); the pore radius dependence of the perturbation zone radius (b); the pore radius dependence of the BLM deformation wavelength (c). Curves 1: reference BLM. Curves 2: BLM with the hydrophobic thickness of 22 Å. Curves 3: BLM similar with the reference BLM, but with a polar headgroup area a_0 of 44 Å^2. The information in the Fig. 4 are supplemented by those from the Table 1.

If the deformation wavelength has its value in the greater value interval, $\lambda \in [\lambda_0 \div \lambda_{1M}] = [117.0 \div 125.2]$ Å, then a larger pore will be generated. Its radius will be in the following interval: $[r_{p0} \div r_{pM}] = [10.3 \div 15.0]$ Å. If the radius magnitude of the deformation zone of the collective thermal motion will be embedded in the following non-bijection interval: $[R_1 \div R_2] = [36.5 \div 37.1]$ Å, then it is possible to appear an open pore or a closed one. The magnitude of deformation will determine which of the two pores will be generated.

Following the Table 1, one can notice that the deformation wavelength has its value in the smaller value interval, $\lambda \in [\lambda_{1m} \div \lambda_m] = [112.4 \div 111.4]$ Å, then the closed pore is characterized by ratio d/h. Here, d is the magnitude of the distance on which the pore's surfaces (i.e. envelopes) are in a direct contact, and h is the half of the thickness of the hydrophobic zone. In our case, $d/h \in [0.10 \div 0.94]$. If the deformation wavelength has its value in the greater value interval, $\lambda \in [\lambda_{1M} \div \lambda_2] = [125.2 \div 130.9]$ Å, the open pore will appear. Its radius pertains to the interval: $[r_{pM} \div r_{p2}] = [15.0 \div 16.9]$ Å. The one-to-one correspondence interval between λ and R is divided in two sub-intervals. The first one is $R \in [R_2 \div R_c] = [37.1 \div 69.9]$ Å and it is in correspondence with the following wavelength interval: $\lambda \in [\lambda_2 \div \lambda_c] = [130.9 \div 275.7]$ Å. In this case, a single open stable pore will appear. The second interval: $R \in [R_c \div R_r] = [69.9 \div 96.5]$ Å is correspondent to another wavelength interval: $\lambda \in [\lambda_c \div \lambda_r] = [275.7 \div 384.1]$ Å. In this case, an open unstable pore will appear that will evolve towards the BLM rupture.

On the curves describing the dependence of the wavelength of deformation of the perturbing zone radius, vertical bars are figured. The parts of the curves situated at the right of these bars describe the values of λ and R for which the closed pores (zipper pores) are formed.

7.1 The effect of lipid molecule nature

Planar BLM with a high temporal stability are generally obtained by a single species of lipid molecules. We shall analyse such a situation. Therefore, the BLM will be characterised by: the thickness of the hydrophobic core, the thickness of the polar group zone, the electrical state and dipolar orientation of the polar groups, the BLM area occupied by a single lipid molecule equal to that of the hydrophobic chains, and the cross sectional area of a polar headgroup.

Taking into account BLMs differing by the reference BLM by the hydrophobic zone (h = 22 Å), one can study the effect of the hydrophobic zone thickness both on the conditions of pore formation and on the pore magnitude (Fig. 4, curves 3 and Table 1, row 2).

The BLM thickness increase has a slight effect on the magnitude of pore radius. This effect can be observed only in the case of the small pores, whose radii are decreasing. Instead, this influence of the thickness increase is stronger

on the conditions of pore generation. As it can be easily seen from the Table 1, the pore formation, in the case h = 22 Å, is effective when the perturbed zone radius and the corresponding BLM deformation wavelength have great values.

In the case of a critical radius equal to 44 Å ($r_c = 2h$) the small pore radius is decreasing, the pores with larger radius are not affected, while the closing distance of the closed pores is increasing.

The cross-sectional area of the polar headgroup determines indirectly the deformation energy by means of the number of lipid molecules, which must participate to the collective thermal motion, in order to assure the energy required by BLM deformation. In order to appreciate the effect of the area magnitude of polar headgroups on the pore formation, we have approached a BLM, similar in its thickness with the reference BLM, but differing by this one in the cross section area of lipid molecules which, in this case, was of 44 Å^2.

The increasing of the polar headgroup area determines an increase both of the zone magnitude of the collective thermal motion (implicitly, of the number of the lipid molecules involved) and of the magnitude of BLM deformation. Nevertheless, the open pore radius is decreasing, but the closing distance of the closed pore is increasing (Fig. 4, curve 2 and Table 1, row 3).

7.2 Temperature effect

It is evident, that by the temperature raising, the average thermal energy of lipid molecules is increasing. Because, in our case, the thermal energy is the single source of energy involved in BLM deformation, it results that the number of the lipid molecules, which simultaneously participate to the BLM perturbation, must also decrease as the temperature is increasing. Consequently, the radius of the zone occupied by these lipid molecules will decrease, too. This

Table 2. The radia of the collective thermal motion perturbation, the wavelengths of BLM deformation and the radia of pores, in the case of the reference BLM (T = 300 K) and of other two different BLMs for T = 290 K and T = 310 K. R, λ and r are measured in Å. N_m is the minimum number of molecules participating to the collective thermal motion. d/h is the close ratio of the closed pores. In the last column, Cv indicates the curve number within the Fig. 5.

$T(K)$	N_m	$R_m \div R_1$	$\lambda_0 \div \lambda_{1m}$	$r_{p0} \div r_{pm}$	$\lambda_0 \div \lambda_{1M}$	$r_{p0} \div r_{pM}$	Fig/Cv
290	113	37.2-37.7	120.1-115.9	9.8-0.3	120.1-128.1	9.8-14.5	5/8
300	105	36.0-36.5	117.0-112.5	10.3-0.8	117.0-125.2	10.3-15.0	5/1
310	99	34.9-35.5	114.2-109.3	10.5-0.8	114.2-123.2	10.5-15.3	5/9
T(K)	N_m	$R_1 \div R_2$	$\lambda_{1m} \div \lambda_m$	d/h	$\lambda_{1M} \div \lambda_2$	$r_{pM} \div r_{p2}$	
290	113	37.7-38.3	115.9-115.0	0.22-0.94	128.1-133.5	14.5-16.4	
300	105	36.5-37.1	112.4-111.4	0.10-0.94	125.2-130.9	15.0-16.9	
310	99	35.5-36.1	109.3-108.3	0.09-0.94	123.3-128.3	15.3-16.9	
T(K)	N_m	$R_2 \div R_c$	$\lambda_2 \div \lambda_c$	$r_{p2} \div r_{pc}$	$R_c \div R_r$	$\lambda_c \div \lambda_r$	$r_{pc} \div r_r$
290	113	38.3-71.3	133.4-315.6	16.4-40.4	71.3-101.5	315.6-397.9	40.4-58.0
300	105	37.1-69.9	130.9-275.7	16.9-40.4	69.9- 96.4	275.7-384.1	40.4-53.1
310	99	36.1-55.1	128.2-219.5	16.9-32.1	–	–	–

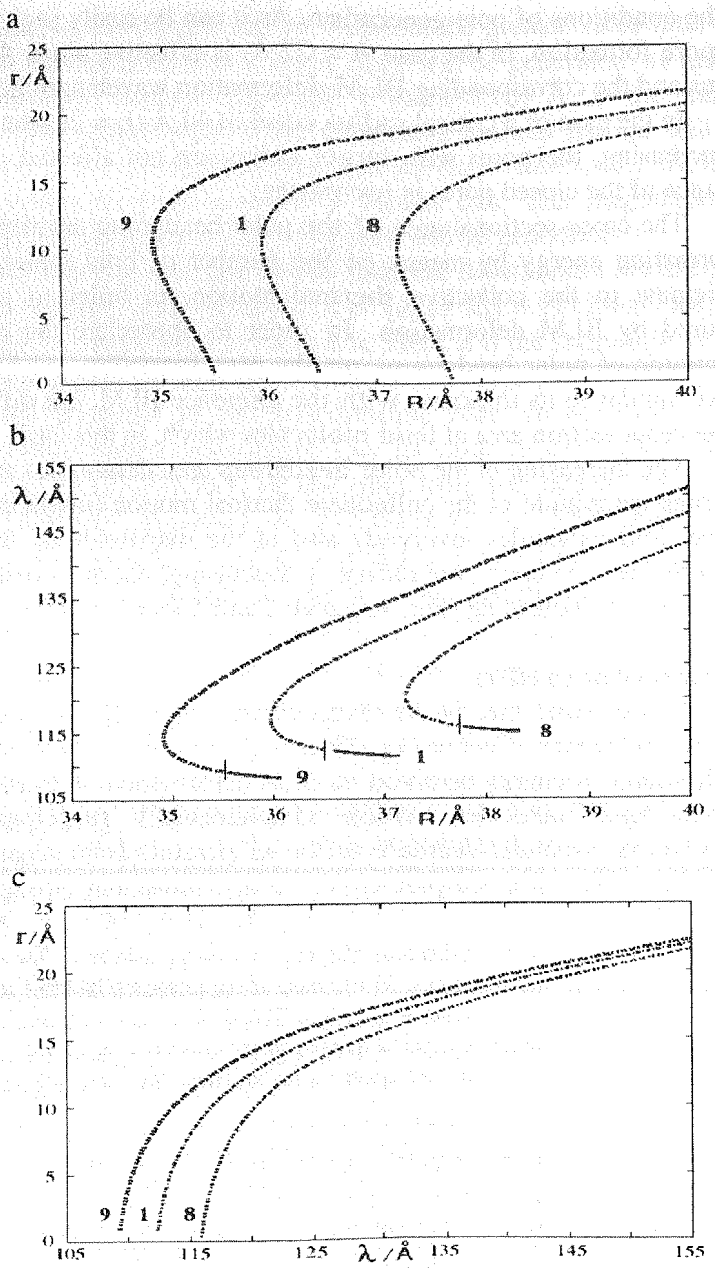

Fig. 5 The graphs, in the case of reference BLM, for: the deformation wavelength dependence of the perturbation zone radius (a); the pore radius dependence of the perturbation zone radius (b); the pore radius dependence of the BLM deformation wavelength (c). Curves 8: $T = 290$ K. Curves 1: $T = 300$ K. Curves 9: $T = 310$ K. The information in the Fig. 5 are supplemented by those from the Table 2.

conclusion is confirmed by the solutions of the Eq. (22) for the reference BLM, in the case of two temperatures 290 K and 310 K, under the phase transition temperature (Fig. 5 and Table 2). In exchange, the open pore radius is increasing with temperature, while the closed pore closing distance is decreasing.

7.3 Effect of the intermolecular forces

In this section we shall approach the effect of: a) the variation of the splay elastic properties, b) the elastic compression properties, and c) the surface tension.

a) The effect of the variation of the splay elastic properties. Molecular rotation energy against the normal direction to the BLM is known as the splay energy, being characterised by the splay elastic constant, K_1. This energy depends on the interaction between BLM lipid molecules. The splay constant values, experimentally determined for the glycerolmonooleat BLM, are belonging to the following interval: $[0.93 \div 2.17] \times 10^{-11}$N. The values of the splay constant for phosphatidilcholine, are belonging to the same interval [16].

In order to appreciate the role of the splay properties on the pore formation, this elastic constant was modified, namely: the minimal value of the splay elastic constant, $K_1 = 0.93 \times 10^{-11}$N, of the reference BLM, was replaced by the maximal value, $K_1 = 2.17 \times 10^{-11}$N. It can be observed that all calculated values (R, λ, r_p) are shifted to greater values, while the closing distance of the closed pore is shifted towards smaller values (Fig. 6, curves 6 and Table 3, row 2). The influence of splay constant increase is stronger on the open pore radius.

b) The effect of the elastic compression properties. The experimental value of the compression constant, in the case of BLM composed of double chain lipids without solvent, is $\overline{B} = 5.36 \times 10^7$ Nm^{-2}, while in the case of the same BLM, but containing solvent, is $\overline{B} = 5.75 \times 10^4$ Nm^{-2}.

Compressibility properties have the strongest effect on the transbilayer pore formation. If the Eq. (22) is solved, in the case of $\overline{B} = 1.5 \times 10^7$ Nm^{-2}, it results that the dependence between λ and R becomes monotonically decreasing, which eliminates the possibility of pore appearance with two geometric states (forms). Both the radius of the perturbed zone and the wavelength of the deformation are strongly decreasing. The pores that appear are either open pores, with larger radii, or closed ones, with smaller closing distances (Fig. 6, curves 5 and Table 3, row 3). The decreasing of compression constant eliminates the possibility of the membrane rupture, as a consequence of the pore formation. On the other hand, the modification of the compression elastic constant, from the value, $\overline{B} = 5.36 \times 10^7$ Nm^{-2} to the value, $\overline{B} = 1.5 \times 10^7$ Nm^{-2}, determines a modification of the curves: $\lambda = \lambda(R)$, $r_p = r_p(R)$, $r_p = r_p(\lambda)$. There is a critical value, $B_c = 14.5 \times 10^7$ Nm^{-2}, beyond which these changes are taking place. For the values of $\overline{B}$ greater than this critical value, the wavelength dependence of the

perturbed zone radius has no one-to-one correspondence. From the Fig.6, it results that only the curve "branch" of the greater values of the wavelength are influenced by the increasing of the compression elastic constant. The width of the non-univocity interval is decreasing with the increasing of the $\overline{B}$ constant, so that, for $\overline{B} = B_c = 14.5\times10^7$ Nm^{-2}, the superior branch of the curve (representing the wavelength dependence of the perturbed zone radius), becomes parallel with $O\lambda$ axis. This is equivalent with an uncertainty of the radius dependence of the wavelength.

For the values of $\overline{B}$ smaller than the critical value ($\overline{B} < B_c$) the dependence of wavelength of the radius, R, becomes of a univocity type, and the interval of the wavelength spectrum is narrowing with the decreasing of $\overline{B}$. For values of $\overline{B}$ around the value, $\overline{B} = 12.5\times10^6$ Nm^{-2}, the sensitivity of wavelength dependence of R is very weak. The compression elastic constant can be also modified in the case when the double chain lipids of BLM are replaced by lisophospholipids.

c) The effect of surface tension. The coefficient of surface tension, characterizing the molecular interactions at the separation surface of two non-miscible media, is depending of the composition of these two media. In the case of BLM, the surface tension coefficient is dependent of the pH of the BLM adja-

Table 3. The values of the zone radia of collective thermal motion perturbation and of the wavelength BLM deformation, in the case of the reference BLM and of other three bilayers which differ from this one by: the elastic splay constant, $K_1 = 2.17\times10^{-11}$N, the compression constant, $\overline{B} = 1.5\times10^7$ Nm^{-2}, and by surface tension coefficient, $\gamma = 2.4\times10^{-4}$Nm^{-1}, respectively. The parameters R, λ and r are measured in Å. N_m is the minimum number of molecules participating simultaneously to the collective thermal motion. In the last column, Cv indicates the curve number within the Fig. 6. d/h is the close ratio of the closed pores.The information from the Table 3 are supplemented by those in the Fig. 6.

N_m	$R_m \div R_1$	$\lambda_0 \div \lambda_{1m}$	$r_{p0} \div r_{pm}$	$\lambda_0 \div \lambda_{1M}$	$r_{p0} \div r_{pM}$	Fig/Cv
105	36.0-36.5	117.0-112.5	10.3-0.8	117.0-125.2	10.3-15.0	6/1
156	43.7-44.5	142.4-136.7	12.5-1.0	142.4-152.3	12.5-18.2	6/6
98	34.8-35.3	113.1-108.5	9.9-0.8	113.1-120.9	9.9-14.5	6/7
51	25.0-28.2	99.6- 86.7	4.6-0.6	–	–	6/5
N_m	$R_1 \div R_2$	$\lambda_{1m} \div \lambda_m$	d/h	$\lambda_{1M} \div \lambda_2$	$r_{pM} \div r_{p2}$	
105	36.5-37.1	112.4-111.4	0.10-0.94	125.2-130.9	15.0-16.9	
156	44.5-45.2	136.7-135.5	0.10-0.94	152.3-158.2	18.2-20.2	
98	35.3-35.8	108.5-107.7	0.10-0.94	120.9-125.3	14.5-16.0	
51	28.2-28.5	86.7- 85.7	0.09-0.94	–	–	
N_m	$R_2 \div R_c$	$\lambda_2 \div \lambda_c$	$r_{p2} \div r_{pc}$	$R_c \div R_r$	$\lambda_c \div \lambda_r$	$r_{pc} \div r_r$
105	37.1-69.9	130.9-275.7	16.9-40.4	69.9- 96.4	275.7-384.1	40.4-53.1
156	45.2-70.4	158.2-277.0	20.2-40.4	70.4-111.4	277.0-444.5	40.4-14.9
98	35.8-68.4	125.3-271.7	16.0-40.4	68.4- 81.8	271.7-326.1	40.4-47.6
51	–	–	–	–	–	–

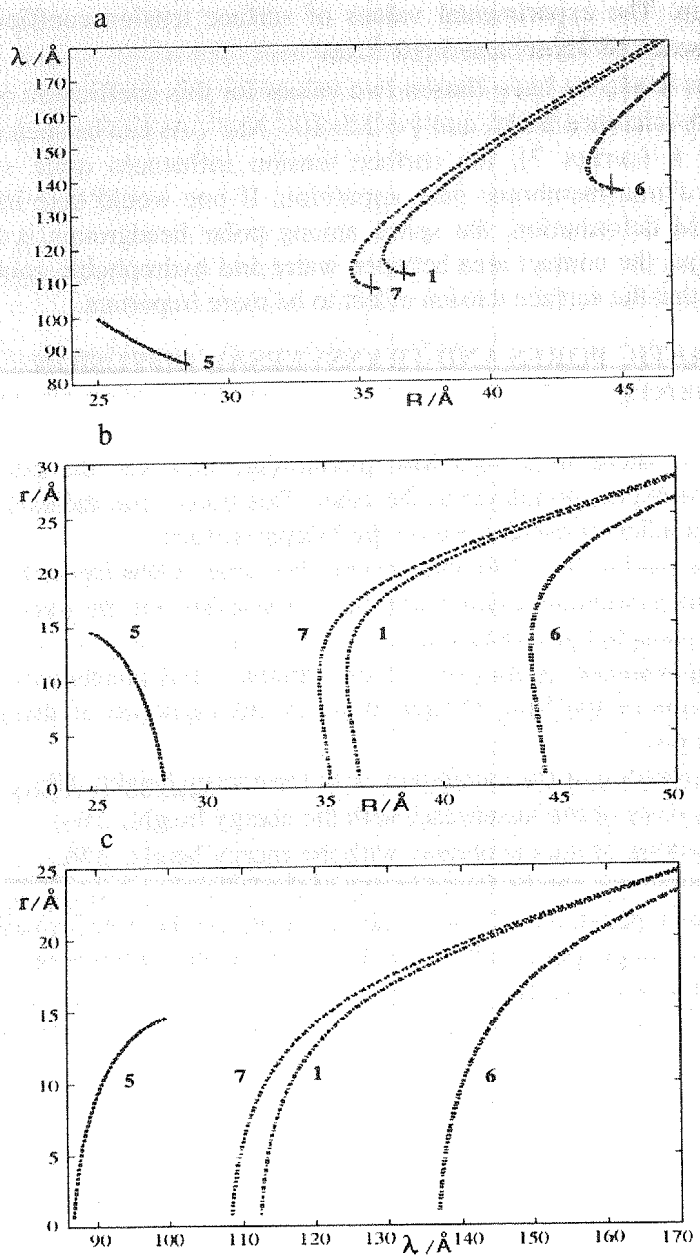

Fig. 6 The graphs, for: the deformation wavelength dependence of the perturbation zone radius (a); the pore radius dependence of the perturbation zone radius (b); the pore radius dependence of the BLM deformation wavelength (c). Curves 1: reference BLM. Curves 5: BLM with the elastic compression coefficient, $\overline{B} = 1.5\times10^{7}$ Nm^{-2}. Curves 6: BLM with the elastic splay coefficient, $K_1 = 2.17\times10^{-11}$N. Curves 7: BLM with the surface tension coefficient, $\gamma = 2.4\times10^{-4}$ Nm^{-1}.

cent medium. The experimental values of surface tension coefficient, γ, are situated between 10^{-8} Nm^{-1} and 5×10^{-2} Nm^{-1}.

In this work, we have chosen two values for this coefficient: $\gamma = 15\times10^{-4}$ Nm^{-1}, for the reference BLM, and $\gamma = 2.5\times10^{-4}$ Nm^{-1}. As can be seen from Table 3 and Fig. 6 (curves 7), the surface tension influences quite slightly the conditions of transmembrane pore apparition. If one would take into account that by BLM deformation, the space among polar headgroups is increasing, favouring thus the contact area between water and hydrophobic zone, it would be possible that the surface tension effect to be more important.

8. STOCHASTIC PORES AND TRANSVERSAL DIFFUSION COEFFICIENTS

Even if there is a very low probability, however the phospholipids translocate from one monolayer to the other. This transversal diffusion is caused by their perpendicular oscillations on the bilayer surface.

In this section, we demonstrate that the pores following self-oscillations of the bilayer membrane might represent a possibility for the passive flip-flop diffusion of phospholipid molecules.

The appearance of statistical pores through lipid membranes due to the self-oscillations of the lipid bilayer involves the existence of three energetic barriers [56] for:

1) perforation of the membrane, with the energy height, ΔW_1;
2) recovery of the membrane, with the energy height, ΔW_2;
3) breaking of the membrane, with the energy height, ΔW_3.

The membrane can be found in one of the following states [56]:
-state 1, without pores, namely in the phase preceding the pore formation;
-state 2, with a single pore on it, regardless the diameter of the pore;
-state 3, the broken membrane.

The scheme for the kinetics of state transitions of the membrane is the following:

$$1 \underset{k_2}{\overset{k_1}{\rightleftarrows}} 2 \xrightarrow{k_3} 3 \tag{35}$$

with the rate constants:

$$k_1 \approx \exp(-\beta\Delta W_1) \tag{36}$$
$$k_2 \approx \exp(-\beta\Delta W_2) \tag{37}$$
$$k_3 \approx \exp(-\beta\Delta W_3) \tag{38}$$

where $\beta = 1/kT$.

If we denote the probabilities that at a given time the membrane is found to be in the states 1, 2 and 3, by $P_1(t)$, $P_2(t)$ and $P_3(t)$, respectively, then the kinetic description of this system is given by the following system of equations:

$$dP_1 / dt = k_2 P_2(t) - k_1 P_1(t) \tag{39}$$
$$dP_3 / dt = k_3 P_2(t) \tag{40}$$
$$P_1(t) + P_2(t) + P_3(t) = 1 \tag{41}$$

with the initial conditions: $P_1(0) = 1$, $P_2(0) = 0$, $P_3(0) = 0$.

Let us introduce a dimensionless rate variable defined by the following expression:

$$\tau = (k_1 + k_2 + k_3)t \tag{42}$$

Then, the probabilities to find each of the three states are:

$$P_1 = [(x_1 + v)\exp(x_2\tau) - (x_2 + v)\exp(x_1\tau)]/\, y \tag{43}$$
$$P_2 = v[\exp(x_1\tau) - \exp(x_2\tau)]/\, y \tag{44}$$
$$P_3 = 1 - [x_1 \exp(x_2\tau) - x_2 \exp(x_1\tau)]/\, y \tag{45}$$

with the auxiliary relations:

$$v = k_1 (k_1 + k_2 + k_3)^{-1} \tag{46}$$
$$u = k_1 k_2 (k_1 + k_2 + k_3)^{-2} \tag{47}$$
$$y = \sqrt{1 - 4u} \tag{48}$$
$$x_1 = (y - 1)/2 \tag{49}$$
$$x_2 = -(y + 1)/2 \tag{50}$$

We can say that the distribution function of the lifetime of the pore is:

$$F(\tau) = P_3(\tau) \tag{51}$$

Thus, the probability density has the following expression:

$$f(\tau) = dF(\tau)/d\tau = u\exp(x_1\tau)[1 - \exp(-y\tau)]/\, y \tag{52}$$

Finally, the mean lifetime, $\bar{\tau}$, of the pore is equal to:

$$\bar{\tau} = \int_0^\infty \tau f(\tau) d\tau = 1/u \tag{53}$$

The mean number, $\bar{n}$, of pores is equal to the probability of a pore appeared on a stable (unbroken) membrane [58]:

$$\bar{n} = P_2/(P_1 + P_2) = \nu[\exp(y\tau) - 1]/x_1 \tag{54}$$

The number of phospholipid molecules that cross the median plane of the bilayer through statistical pores is equal to:

$$dN_{ff} = n dN_t \tag{55}$$

where dN_t is the number of molecules that perform a translocation through the pore. Therefore, the flip-flop diffusion coefficient is $D_{ff} = nD_l$.

Taking into consideration that:

$$n = \lim_{a\to\infty} \frac{1}{a} \int_0^a n(\tau) d\tau = \nu/|x_2| \tag{56}$$

we obtain:

$$n \approx k_1/(k_1 + k_2 + k_3) \tag{57}$$

From the results of Ref. [56], the energy barriers for ΔW_1, ΔW_2 and ΔW_3 are 91.2, 65.6 and 2,090.1 kT, respectively. Then it was obtained $n = exp(-25)$. Because the lateral diffusion coefficient, D_l, of the phospholipids at the surface of the planar bilayer is in the order 10^{-12} m^2s^{-1}, this gives the value $D_{ff}=10^{-12}exp(-25) = 10^{-23}$ m^2s^{-1}. If we consider that formula for D_{ff}, is similar to that for the translation diffusion:

$$D_{ff} = \overline{r^2}/4\tau \tag{58}$$

and adopt the model of jumps in an ordered 2-dimensional network, then

$$d = \sqrt{\overline{r^2}} \tag{59}$$

will be the thickness of the hydrophobic domain of the lipid bilayer. Here and henceforth, τ is the duration of the jump from one monolayer into the other.

If we consider a lipid bilayer with a thickness of 30 Å, then the translocation time, τ, is:

$$\tau = \overline{r^2} / D_{ff} = 2.25 \times 10^5 \text{ s} \tag{60}$$

It is interesting to observe that this is result in the same order of magnitude as the lifetime of phospholipids in a lipid bilayer. This calculation demonstrates the passive flip-flop translocation of phospholipids across a statistical pore formed in a lipid membrane is a very rare but detectable event [91].

This mechanism for the translocation of phospholipids from one monolayer to another one is possible because: (1) there are oscillations of the lipid bilayer surface due to thickness fluctuations [56]; (2) there are perpendicular oscillations of the phospholipids on the monolayer plane [92].

In addition, the oscillations into the neighbour water medium are forestalled by the hydrophobic effect within the hydrocarbon domain, which appear via image forces due to polar headgroups of phospholipids.

9. CONCLUSIONS

Since their use for the first time as the reconstitution *in vitro* of cell membrane structure [93], BLMs were and continue to be the most suited artificial membrane models in numerous experiments that supplied the extremely important information necessary to a better understanding of the very intricate life processes occurring in living cells [94].

Among the membrane related phenomena, the membrane transport occupies a central role. It is important to emphasize that in this transport mechanism, among other complex structures (e.g. ionic pumps, ionic channels, etc.) the different types of pores are involved, too.

We tried to demonstrate that the general theory of continuous elastic media can predict the generation of all types of pores due to the BLM thermal thickness fluctuations.

Our results are explaining both the pore formation and their properties and, besides are confirming the existence of a new mechanism of transbilayer pore formation.

The values of the open pore radii, obtained by us, are in agreement with those encountered in the literature, while the closed pore formation confirms an old hypothesis concerning the existence of water "little threads" into the hydrophobic region of the lipid bilayers [95].

Taking into account that the thermal energy necessary to provoke BLM deformation is proportional to R^2, it results that the closer to R_m is the radius of the collective thermal motion zone, the greater is the probability of a pore appearance.

The closed pores can be very stable due to the coupling between the polar headgroup dipoles, the space between the polar headgroups being filled with a row of water molecules. Practically, the closed pore radius is not zero.

The mechanism of pore formation is based on the variation of BLM thickness due to the collective thermal motion, but it doesn't exclude the surface defects induced by lateral thermal motions. However, the mechanism of pore formation by thermal fluctuations still continue to be a matter of challenge and interesting future developments.

REFERENCES

[1] W. Helfrich, Z. Naturforsch., 28 (1973) 693.
[2] E. A. Evans and R. Skalak, Mechanics and Thermodynamics of Biomembranes, CRC Press, Boca Raton, 1980.
[3] S. B. Hladky and D. W. R. Gruen, Biophys. J., 38 (1982) 251.
[4] I. R. Miller, Biophys. J., 45 (1984) 643.
[5] S. B. Hladky, Biophys. J. 45 (1984) 645.
[6] E. Evans and W. Rawicz, Phys. Rev. Letters 64 (1990) 2094.
[7] J. N. Israelachvili, Intermolecular and Surface Forces, 2nd edn, Academic Press, New York, 1992.
[8] A. Ben-Shaul, In: R. Lipowsky and E. Sackmann (eds.), Structure and Dynamics of Membranes, 2nd edn, vol 1, Elsevier, Amsterdam, 1995.
[9] S. May, J. Chem. Phys., 103 (1995) 3839.
[10] S. May, J. Chem. Phys., 105 (1996) 8314.
[11] W. Rawicz, K. C. Olbrich, T. McIntosh, D. Needham and E. Evans, Biophys. J. 79 (2000) 328.
[12] E. H. DeLacey and J. Wolfe, Biochim. Biophys. Acta 692 (1982) 425.
[13] I. R. Elliott, D. Needham, J. P. Dilger and D. A. Haydon, Biochim. Biophys. Acta 735 (1983) 95.
[14] O. G. Mouritsen and M. Bloom, Biophys. J. 36 (1984) 141.
[15] J. R. Abney and J. C. Owicki, In: A. Watts and J. De Pont (eds.), Progress in Protein-Lipid Interactions, Elsevier, New York, 1985.
[16] H. W. Huang, Biophys. J., 50 (1986) 1061.
[17] P. Helfrich and E. Jakobsson, Biophys. J., 57 (1990) 1075.
[18] S. M. Gruner, In: L. Pelity (ed.), Biologically Inspired Physics, Plenum Press, New York, 1991.
[19] N. Dan, P. Pincus and S. A. Safran, Langmuir 9 (1993) 2768.
[20] M. F. Brown, Chem. Phys. Lipids 73 (1994) 159.
[21] N. Dan, A. Berman, P. Pincus and S. A. Safran, J. Phys. II France 4 (1994) 1713.
[22] A. Ring, Biochim. Biophys. Acta, 1278 (1996) 147.
[23] C. Nielsen, M. Goulian and O. S. Andersen, Biophys. J., 74 (1998) 1966.
[24] S. May and A. Ben-Shaul, Biophys. J., 76 (1999) 751.
[25] S. May, Eur. Biophys. J., 29 (2000) 17.
[26] M. M. Sperotto, Eur. Biophys. J., 26 (1997) 405.
[27] K. S. Kim, J. Neu and G. Oster, Biophys. J., 75 (1998) 2274.
[28] F. Brochard and J. F. Lennon, J. Physique, 36 (1975) 1035.
[29] R. Waugh and E. A. Evans, Biophys. J., 26 (1979) 115.
[30] T. M. Fischer, Biophys. J., 63 (1992) 1328.
[31] L. Miao, U. Seifert, M. Wortis and H.-G. Döbereiner, Phys. Rev., E 49 (1994) 5389.
[32] R. T. Tranquillo and W. Alt, J. Math. Biol., 34 (1996) 361.
[33] L. Movileanu and D. Popescu, BioSystems, 36 (1995) 43.
[34] L. Movileanu and D. Popescu, J. Biol. Systems, 4 (1996) 425.

[35] D. W. R. Gruen, S. Marcelja and V. A. Parsegian, In: A. S. Perelson, C. Delisi and F. W. Wiegel (eds.), Cell Surface Dynamics, Dekker, New York, 1984.
[36] J. N. Israelachvili, S. Marcelia and R. G. Horn, Quarterly Rev. Biophys., 13 (1980) 121.
[37] D. Popescu, Biochim. Biophys. Acta, 1152 (1993) 35.
[38] D. Popescu, Biophys. Chem., 48 (1994) 369.
[39] M. H. Saier, Jr. and C. D. Stiles, Biological Membranes, Springer Verlag, New York, 1975.
[40] D. Popescu and C. Rucareanu, Mol. Cryst. Liq. Cryst., 25 (1992) 339.
[41] E. Sackmann, In: R. Lipowsky and E. Sackmann (eds.), Structure and Dynamics of Membranes, Elsevier/North-Holland, Amsterdam, 1995.
[42] J. C. Shillcock and U. Seifert, Biophys. J., 74 (1998) 1754.
[43] J. F. Nagle and S. Tristram-Nagle, Curr. Op. Struct. Biol., 10 (2000) 474.
[44] C. Tanford, The Hydrophobic Effect: Formation of Micelles and Biological Membranes, John Wiley, New York, 1980.
[45] D. Popescu and G. Victor, Bioelectrochem. Bioenerg., 25 (1991) 105.
[46] M. Shinitzki and P. Hencart, Int. Rev. Cytol., 60 (1979) 121.
[47] I. G. Abidor, V. B. Arakelyan, I. V. Chernomondik, Yu. A. Chizmadzhev, V. F. Pastushenko and M. R. Tarasevich, Bioelectrochem. Bioenerg., 6 (1979) 37.
[48] R. Benz, O. Fröhlich, P. Lauger and M. Montal, Biochim. Biophys. Acta, 394 (1975) 323.
[49] R. J. Cherry and D. Chapman, J. Mol. Biol., 40 (1969) 19.
[50] J. P. Dilger, Biochim. Biophys. Acta, 645 (1981) 357.
[51] D. Popescu, and G. Victor, Biochim. Biophys. Acta, 1030 (1990) 238.
[52] L. Movileanu, D. Popescu and M. L. Flonta, J. Mol. Struct., 434 (1998) 213.
[53] L. Movileanu, D. Popescu, G. Victor and G. Turcu, Bull. Math. Biol., 50 (1997) 60.
[54] K. Jorgensen and O. G. Mouritsen, Biophys. J., 95 (1995) 942.
[55] K. Jorgensen, M. M. Sperotto, O. G. Mouritsen, J. H. Ipsen and M. J. Zuckermann, Biochim. Biophys. Acta, 1152 (1993) 135.
[56] D. Popescu, C. Rucareanu and G. Victor, Bioelectrochem. Bioenergetics, 25 (1991) 91.
[57] D. Zhelev and D. Needham, Biochim. Biophys. Acta, 1147 (1993) 89.
[58] D. Popescu and D. G. Margineanu, Bioelectrochem. Bioenerg., 8 (1981) 581.
[59] J. C. Shillcock and D. H. Boal, Biophys. J., 71 (1996) 317.
[60] J. D. Moroz and P. Nelson, Biophys. J., 72 (1997) 2211.
[61] J. C. Weaver and Yu. A. Chizmadzhev, Bioelectrochem. Bioenerg., 41 (1996) 135.
[62] G. Saulis, Biophys. J., 73 (1997) 1299.
[63] W. Sung and P. J. Park, Biophys. J., 73 (1997) 1797.
[64] E. Neumann, S. Kakorin and K. Toensing, Bioelectrochem. Bioenerg., 48 (1999) 3.
[65] L. K. Tamm, A. Arora and J. H. Kleinschmidt, J. Biol. Chem., 276 (2001) 32399.
[66] L. Movileanu, S. Cheley, S. Howorka, O. Braha and H. Bayley, J. Gen. Physiol., 117 (2001) 239.
[67] S. Howorka, L. Movileanu, X. Lu, M. Magnon, S. Cheley, O. Braha and H. Bayley, J. Am. Chem. Soc., 122 (2000) 2411.
[68] L. Movileanu, S. Howorka, O. Braha and H. Bayley, Nature Biotechnol., 18 (2000) 1091.
[69] L. Movileanu and H. Bayley, Proc. Natl. Acad. Sci. USA, 98 (2001) 10137.
[70] S. Howorka, L. Movileanu, O. Braha and H. Bayley, Proc. Natl. Acad. Sci. USA, 98 (2001) 12996.
[71] J. Konisky, Ann. Rev. Microbiol., 36 (1982) 125.
[72] R. Cassia-Moura, Bioelectrochem. Bioenerg. 32 (1993) 175.
[73] P. K. Kienker, X. Qiu, S. L. Slatin, A. Finkelstein, and K. S. Jakes, J. Memb. Biol., 157 (1997) 27.

[74] R. Cassia-Moura, A. Popescu, J. R. A. Lima, C. S. Andrade, L. S. Ventura, K. S. A. Lima and J. Rinzel, J. Theor. Biol., 206 (2000) 235.
[75] E. Wisse and D. L. Knook, In: Progress in Liver Diseases, vol. VI. H. Popper and F. Schaffner (eds.), Straton, Grune, 1979.
[76] D. Popescu, L. Movileanu, S. Ion and M. L. Flonta, Phys. Med. Biol., 45 (2000) N157.
[77] H. T. Tien and A. L. Ottova, J. Membr. Sci., 4886 (2001) 1.
[78] S. J. Singer and G. L. Nicholson, Science, 175 (1972) 720.
[79] P. G. de Gennes, The Physics of Liquid Crystals. Clarendon Press, Oxford, 1974.
[80] I. Pascher, M. Lundmark, P. G. Nyholm and S. Sundell, Biochim. Biophys. Acta, 1113 (1992) 339.
[81] H. Hauser, I. Pascher, R. H. Pearson and S. Sundell, Biochim. Biophys. Acta, 650 (1981) 21.
[82] C. H. Huang and J. T. Mason, Biochim. Biophys. Acta, 864 (1986) 423.
[83] D. Popescu and G. Victor, Biophys. Chem., 39 (1991) 283.
[84] J. D. Litster, Phys. Lett., 53A (1975) 711.
[85] J. C. Weaver and R. A. Mintzer, Phys. Lett., 86A (1981) 57.
[86] B. L. Silver, The Physical Chemistry of Membranes, Allen & Unwin, London, 1985.
[87] S. H. White, Biophys. J., 23 (1978) 337.
[88] E. Neher and H. Eibl, Biochim. Biophys. Acta, 464 (1977) 37.
[89] H. Engelhardt, H. P. Duwe and E. Sackman, J. Physique Lett., 46 (1985) L395.
[90] M. B. Schneider, J. T. Jenkins and W. W. Webb, J. Physique, 45 (1984) 457.
[91] L. Movileanu, D. Popescu, G. Victor and G. Turcu, BioSystems, 40 (1997) 263.
[92] M. Shinitzky, Biomembranes. Physical Aspects, Balaban Publishers VCH, Weinheim, 1993.
[93] P. Mueller, D. O. Rudin, H. T. Tien, W. C. Wescott, Nature 194 (1962).
[94] H. T. Tien and A. Ottova-Leitmannova, Membrane Biophysics as Viewed from Experimental Bilayer Lipid Membranes. Elsevier, Amsterdam and New York, 2000.
[95] H. Trauble, J. Membr. Biol., 4 (1971) 193.